

TABLE 3: A summary of the performance of eGFR equations in critically ill patients with AKI, whose  $^{4}\text{CrCl}$  was less than  $60 \text{ mL} \cdot \text{min}^{-1}$  per  $1.73 \text{ m}^2$  and whose urine output was greater than  $0.2 \text{ mL} \cdot \text{kg}^{-1}$  per min during the study period (37 patients).

	$^{4}\text{CrCl}$	1/creatinine	Cockcroft and Gault	aMDRD	MDRD 6	MDRD 7	CKD EPI	Cystatin C1	Cystatin C3	Cystatin C4
Mean eGFR ( $\text{mL} \cdot \text{min}^{-1}$ per $1.73 \text{ m}^2$ )	27.1*	53.4	35.5	33.3	35.5	28.8	32.3	43.2	41.0	39.7
Range ( $\text{mL} \cdot \text{min}^{-1}$ per $1.73 \text{ m}^2$ )	8–51	13–119	11–63	9–87	9–79	8–71	9–80	17–85	16–79	15–79
$r^2$ correlation ( $P < 0.0001$ )	0.64	0.82	0.72	0.75	0.71	0.70	0.70	0.71	0.71	0.70
Bias ( $1.96 \times \text{SD}$ )	-26.3	-8.4	-6.2	-5.4	-1.6	-5.2	-16.1	-13.9	-12.5	
Percentage error (precision)	52	39	56	47	58	57	46	47	42	
Accuracy (%)										
10%	3	16	16	27	16	24	11	14	16	
30% ( $P_{30}$ )	5	46	57	49	70	57	27	30	35	
50%	22	68	78	76	86	81	46	54	59	

\*Measured not estimated.

value) which is perhaps more useful comparison hence its use in this analysis.

A recent study of eGFR performance in renal transplant patients, [39] used Bland-Altman analysis and described the bias of C&G, aMDRD, and MDRD 7 as 15.2, 9.2, and 7.4 and worse than this study. The precision (25.4%, 21.9%, and 20%, resp.) however, was better and within range suggested previously [38]. The percentage of values within 30% of the  $^{4}\text{CrCl}$  ( $P_{30}$ ) (37, 60, and 67.4, resp.) was comparable to the data from this study, and the use of the equations in renal transplant recipients is recommended.

When introduced, the CKD-EPI equation [7] had a bias of  $2.1 \text{ mL} \cdot \text{min}^{-1}$  per  $1.73 \text{ m}^2$  and a  $P_{30}$  of 79.9%, which are better than data presented in this study and comparable only to the MDRD 7 equation.

Using methods based on cystatin C when compared with methods incorporating serum creatinine have shown a higher correlation and improved accuracy in predicting GFR in patients with various degrees of renal function, liver disease, and spinal cord injuries [17]. However, results in patients with diabetes, paediatric patients, and those with early renal impairment did not show a significant difference between cystatin C and creatinine based eGFR, indicating that the performance may be patient population specific [40–43]. Human studies also suggest that cystatin C can predict the development of AKI [44] and the requirement for renal replacement therapy [45], although its superiority over serum creatinine has not been a universal finding [46].

Data presented in this study demonstrate a very broad range of both  $^{4}\text{CrCl}$  and cystatin C measurement across each of the AKIN/RIFLE criteria. Figure 3 shows that serum cystatin C increased with worsening renal function measured by  $^{4}\text{CrCl}$ , but the correlation coefficient is not compelling and the confidence intervals are wide. When originally derived, the equations which incorporate cystatin C showed minimal bias and excellent accuracy with  $P_{30}$  of 81%, 83%, and 89% for cystatin C1, C3, and C4 equations, respectively [16]. These

results were not reproduced in this study and the cystatin C equations actually perform worse than the original MDRD equations in patients with AKI.

## 6. Limitations

Measuring rapid changes in renal function accurately in critically ill patients is difficult and there is no gold standard method. A useful, routine exogenous marker has remained elusive and there are well-described difficulties when interpreting creatinine clearance. Tubular secretion and extrarenal elimination of creatinine increases as GFR deteriorates, thus exaggerating the discrepancy between the clearance of creatinine and true renal function [47]. In addition, serum creatinine concentrations are influenced by muscle mass, protein intake, gender, and age, limiting the precision further. The influence of these factors in the acute setting is not clear. However, over a period of hours and days, as the renal function deteriorates in AKI, one would anticipate that these other factors would remain relatively constant.

Aware of its limitations, in the absence of an accepted gold standard, the  $^{4}\text{CrCl}$  was piloted as a baseline standard. It incorporates both changes in creatinine and urine output and is supported by an evidence base. A small study of eighteen critically ill patients used correlation coefficients to compare clearance of DTPA or inulin (their gold-standard measure) to 2-hour creatinine clearance ( $^{2}\text{CrCl}$ ) [48]. The authors conclude that a  $^{2}\text{CrCl}$  is not an accurate description of inulin clearance, in this population, when the GFR is  $<30 \text{ mL} \cdot \text{min}^{-1}$ . However, reanalysis of the published raw data reveals a correlation coefficient ( $r$ ) between DTPA and 2-hour creatinine clearance of 0.92 ( $P < 0.001$ ) though this is not discussed in the original paper. Perhaps the more encouraging conclusion should include the close relationship with DTPA clearance. There is no mention of urine volume during the study time period and patients with very low DTPA clearances ( $2 \text{ mL} \cdot \text{min}^{-1}$ ) were included.

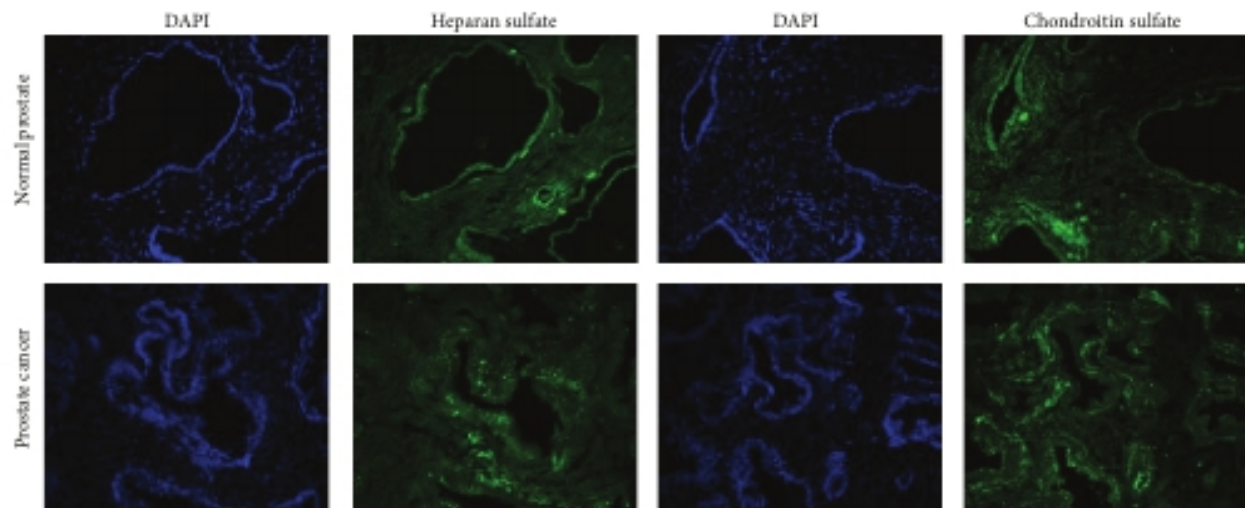


FIGURE 5: Immunohistochemical analysis of glycosaminoglycans in normal prostate tissue and prostate tumour. Heparan sulfate or chondroitin sulfate chains were stained with the appropriate primary antibodies and visualised with FITC-conjugated anti-mouse antibody. The nuclei were counterstained with DAPI. Magnification  $\times 200$ .

perform a real statistical analysis, and all the "means" are very relative. It is a reason why we operate only with tendencies or trends in the analysis of the obtained data.

According to our results, versican was the most stably expressed extracellular proteoglycan in prostate tumours, with the mRNA levels similar to that in normal prostate tissue (Figure 3). It is slightly controversial with the published data on elevated levels of versican protein in prostate cancer, associated with disease progression in early-stage prostate cancer [6, 7]. Possibly, an accumulation of versican in cancer prostate tissue is due to either posttranscriptional activation of versican expression or decreased versican degradation in prostate tumours but not versican regulation at mRNA level.

On decorin expression in prostate cancer, two controversial results were published earlier. It was shown that decorin concentration is increased in the prostatic tissue of men with early-stage prostate cancer [7] or reduced in prostate cancer stroma compared to nonmalignant prostate stroma [8]. Our results outlined a tendency for the decreased decorin expression in prostate tumours (Figure 3); however, a significant individual variation of decorin mRNA levels in different prostate tumours could explain the discrepancy of the experimental data from different sources.

Along with versican and decorin, we identified lumican as a most ubiquitously expressed proteoglycan in prostate tissues with the similar expression levels in normal and pathological tissues. Earlier, the only published paper showed lumican upregulation in BPH when compared with normal prostate tissues [20], with no data for lumican expression in prostate tumours.

Glypican-1 is another proteoglycan, which expression was detected in prostate cancer for the first time. Interestingly, in normal prostate tissue, only epithelial cells expressed glypican-1, whereas prostate tumours displayed significant decrease of glypican-1 expression in cancer epithelial cells and an elevated glypican-1 levels in tumour stroma (Figure 4).

A similar effect was shown for the syndecan-1 expression change in prostate tumours. Syndecan-1 expression was significantly decreased in the cancer epithelial cells but increased in tumour stroma (Figure 4). It was not known for prostate cancer, although was shown for some other cancers. For example, syndecan-1 expression was found mainly in epithelial cells and reduced during malignant transformation of various epithelia, and this loss correlated with the histological differentiation grade of squamous cell carcinomas of the head and neck [22]. The loss of epithelial syndecan-1 and strong stromal syndecan-1 was associated with an unfavorable prognosis in gastric cancer [23].

These results suggest a hypothesis for the controversial data on syndecan-1 expression in prostate cancer. Analysing the literature, one could mention that almost all data on the decreased expression of syndecan-1 were obtained from the cell culture experiments *in vitro*, based on the prostate cancer cell lines of epithelial origin [15, 16]. However, most of the results on the increased expression of syndecan-1 in prostate tumours were shown by immunohistochemistry [12–14]. Possibly, data on simultaneous disappearance of syndecan-1 from prostate cancer epithelial cells and overall increase of syndecan-1 content in tumour stroma could contribute to the understanding of the functional role of syndecan-1 in prostate carcinogenesis.

Totally, our results are in a good agreement with the published data on the proteoglycans expression in prostate cancer and, for the first time, show a common patterns for proteoglycans expression in the normal and tumour prostate tissues.

## 5. Conclusions

Taken together, the results of the present study show that

- normal human prostate tissue expresses a specific set of proteoglycans, localised both in prostate epithelial

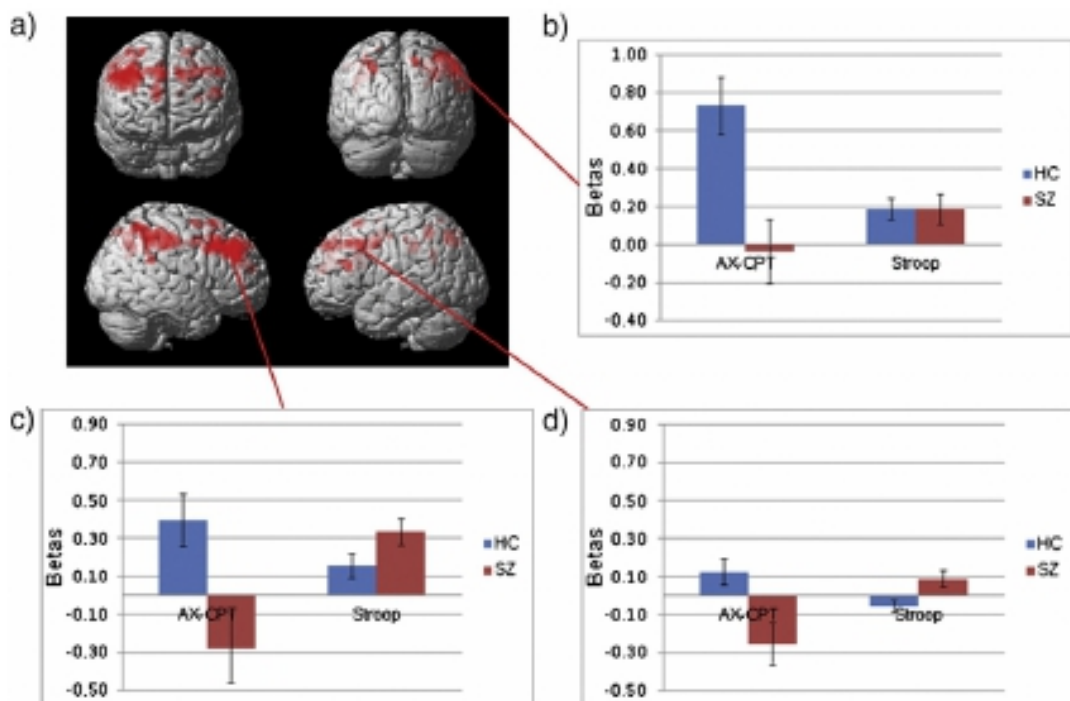


**Fig. 4.** a) Whole-brain thresholded at  $p < .01$  representing the group by task interaction, in which healthy controls (HC) demonstrate greater increases than patients (SZ) in BOLD activity in proactive (AX-CPT B-A) compared to reactive (Stroop I-C) control. The subsequent column graphs represent beta values from the three significant FWE cluster corrected regions representing the group by task interaction: b) inferior parietal cortex, c) right DLPFC, and d) left DLPFC.

on both tasks compared to controls. However, the extent of the performance decrement was much larger for the proactive control measure examining AX hits and BX false alarms compared to the reactive control measure examining Congruent correct and Incongruent error trials. Neuroimaging results revealed robust activation in both reactive and proactive tasks in healthy controls, represented by lateral prefrontal (BA9, BA46, ACC), and inferior parietal regions during the Stroop I-C contrast and prefrontal (BA9, BA46, ACC) and parietal cortex during the AX-CPT B-A contrast. While patients demonstrated activity comparable to controls in the Stroop, activity was markedly reduced during the AX-CPT, with no activity surviving the cluster-wise threshold. More importantly, the interaction analysis of group and task showed that controls increased activity in DLPFC as well as inferior parietal cortex during proactive compared to reactive control, while patients did not show this increase. Taken together these results suggest that schizophrenia individuals demonstrate relatively preserved engagement of the fronto-parietal network during reactive control, but show a reduced ability to increase recruitment in DLPFC and parietal cortex for proactive control.

Additionally, we identified significant relationships between disorganization and both performance and reduced DLPFC activity during proactive control (AX-CPT B-A contrast). These data corroborate the previous work identifying a relationship between disorganization and DLPFC activity (Edwards et al., 2010) and DLPFC connectivity (Yoon et al., 2008). In contrast, no significant relationships were found between disorganization and any metric of reactive control (e.g., Stroop performance, DLPFC I-C activity, or ACC I-C activity). Furthermore, the relationship between disorganization and AX-CPT performance was stronger than the relationship to Stroop performance, suggesting that disorganization is more strongly associated with proactive control processes. These data, taken in the context of the existing literature, suggest that while reactive control deficits have been identified on the Stroop [for review see Henik and Salo, 2004], proactive control processes may be a more robust link to disorganized clinical symptomatology and underlying neuropathophysiology.

These data shed additional light on the pathophysiology of impaired cognition in schizophrenia in several ways. First, they add to an already substantial literature identifying DLPFC impairment in schizophrenia [see Glahn et al., 2005; Minzenberg et al., 2009 for meta-analytic reviews]. Consistent with recent work (Edwards et al., 2010; Perlstein et al., 2003; Yoon et al., 2008), between-group comparisons revealed significantly reduced DLPFC recruitment during the AX-CPT in schizophrenia individuals. Our findings of adequate recruitment of DLPFC and trend level hypoactivation of ACC during reactive control must be considered in the context of some inconsistency in the literature, with some studies of the Stroop revealing PFC hyperactivation in patients (Weiss et al., 2003) and others identifying PFC hypoactivation (Carter et al., 1997; Yucel et al., 2002). These inconsistencies may partly be the result of variability in task design, with some studies including neutral stimuli, presentation in block- or event-related designs, and modifications of the task in which the subject has to explicitly identify whether the word and color are congruent or not as opposed to identifying the ink color with a response. Stage of illness may also play a role as we have previously reported robust ACC decreases using a similar design to the present study in chronic patients (Kerns et al., 2005). Second, our data provide additional support for the dual mechanisms of control theory proposed by Braver et al. (2007). Notably, these data suggest relatively intact reactive control in patients with schizophrenia and imply that prefrontal control deficits in schizophrenia reflect a stronger loading on proactive control processes, reflected in decreased fronto-parietal recruitment. Reduced recruitment of PFC is consistent with the model we presented in a recent review, which theoretically links cellular abnormalities in the PFC with altered inter-regional cortical connectivity, cognitive control dysfunction, and disorganization (Lesh et al., 2011). Sustained activity in the PFC in non-human primates performing working memory tasks depends upon both dopamine (DA) and norepinephrine (NE), modulating neuronal activity through D1 and alpha 2 adrenergic receptors, respectively (Arnsten and Li, 2005; Arnsten et al., 1988; Brozoski et al., 1979; Cai and Arnsten, 1997). GABAergic interneurons are also integral to this process (Gonzalez-Burgos et al., 2010; Lewis et al., 2008). The

TABLE I: The Seventeen Periscapular muscles.

Muscle	Origin	Insertion	Innervation
Serratus anterior	Thoracolumbar fascia, spines of vertebrae T11-T12 and L1-L2	Ribs 9-12, lateral to the angles	Long thoracic nerve
Supraspinatus	Supraspinatus fossa	Greater tubercle of the humerus (highest facet)	Suprascapular nerve
Subscapularis	Medial two-thirds of the costal surface of the scapula (subscapular fossa)	Lesser tubercle of the humerus	Upper and lower subscapular nerves
Trapezius	Medial third of the superior nuchal line, external occipital protuberance, ligamentum nuchae, spinous processes of vertebrae C7-T12	Lateral third of the clavicle, medial side of the acromion, and the upper crest of the scapular spine, tubercle of the scapular spine	Spinal accessory nerve
Teres major	Dorsal surface of the inferior angle of the scapula	Crest of the lesser tubercle of the humerus	Lower subscapular nerve
Teres minor	Upper 2/3 of the lateral border of the scapula	Greater tubercle of the humerus (lowest facet)	Axillary nerve
Triceps brachii long head	Infraglenoid tubercle of the scapula	Olecranon process of the ulna	Radial nerve
Biceps brachii	Short head: tip of the coracoid process of the scapula; long head: supraglenoid tubercle of the scapula	Tuberosity of the radius	Musculocutaneous nerve
Rhomboïd major	Spines of vertebrae T2-T5	Medial border of the scapula inferior to the spine of the scapula	Dorsal scapular nerve
Rhomboïd minor	Inferior end of the ligamentum nuchae, spines of vertebrae C7 and T1	Medial border of the scapula at the root of the spine of the scapula	Dorsal scapular nerve
Coracobrachialis	Coracoid process of the scapula	Medial aspect of midshaft of humerus	Musculocutaneous nerve
Omohyoid (inferior belly)	Upper border of scapula	Hyoid bone	Ansa cervicalis
Latissimus dorsi	Vertebral spines from T7 to the sacrum, posterior third of the iliac crest, lower 3 or 4 ribs, sometimes from the inferior angle of the scapula	Floor of the intertubercular groove	Thoracodorsal nerve
Deltoid	Lateral one-third of the clavicle, acromion, the lower lip of the crest of the spine of the scapula	Deltoid tuberosity of the humerus	Axillary nerve
Levator scapulae	Transverse processes of C1-C4 vertebrae	Medial border of the scapula from the superior angle to the spine	Dorsal scapular nerve
Infraspinatus	Infraspinatus fossa	Greater tubercle of the humerus (middle facet)	Suprascapular nerve
Pectoralis minor	Ribs 3-5	Coracoid process	Medial pectoral nerve

Movement of the glenohumeral joint is controlled by the multiaxial articulation of the concave humeral head with the concave glenoid fossa of the scapula [7]. As it articulates with the glenoid, the humerus rolls, spins, and slides [7] in order to adduct, abduct, extend, flex, and rotate the humerus [7,17]. Changes in the position of the scapula change the relative position of the glenoid fossa and influence glenohumeral joint articulation.

Obligate external rotation of the humerus with abduction prevents impingement of the greater tuberosity on the coracoacromial arch [20]. Internal rotation of the shoulder is mostly a product of motion of the glenohumeral joint, with

minimal contribution from the scapulothoracic articulation. Most people with normal shoulder function will use about 15 degrees of scapulothoracic internal rotation to care for themselves; in the setting of a glenohumeral fusion this increases to 51 degrees of scapulothoracic internal rotation [6].

Full abduction is accomplished via the coordinated movement of several joints. Through the first 30 degrees of abduction, the position of the scapula is relatively unchanged [7] as much of the motion takes place at the glenohumeral joint. With continued abduction, the scapula and clavicle rotate counter-clockwise about an axis that extends from

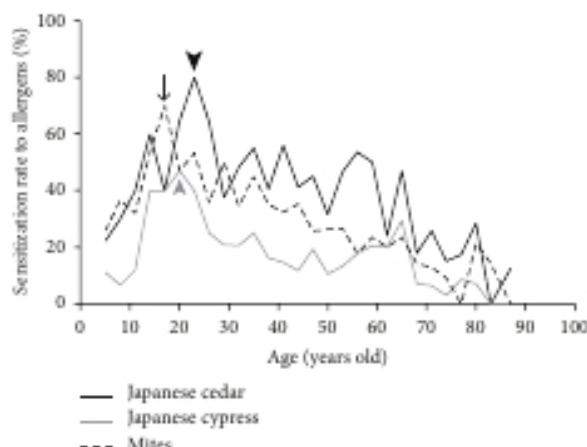


FIGURE 1: The rate of sensitization (determined by RAST) to Japanese cedar, Japanese cypress, and mites was affected by the patient's age. Black arrow head, gray arrow head, and black arrow show the peaks of each rate, respectively.

TABLE 2: Serum total IgE and blood cell eosinophil.

	Total IgE (IU/mL)	Eosinophil cell proportion (%)
Only spring pollens	118 ± 16	4.5 ± 0.4
Only fall pollens	172 ± 93	3.7 ± 1.4
Only perennial allergens	288 ± 51	3.2 ± 0.4
Spring and fall pollens	174 ± 30	5.2 ± 0.9
Spring pollens and perennial allergens	391 ± 67	5.4 ± 0.5
Fall pollens and perennial allergens	—	—
Spring and fall pollens and perennial allergens	878 ± 213	6.1 ± 0.6
No sensitization	120 ± 15	3.1 ± 0.2

The average of total serum IgE levels was highest in 8–17-year olds and decreased with age (Figure 3(a)).

**3.4. Blood Cell Eosinophil Count.** The blood cell eosinophil count was also compared between groups. The eosinophil cell proportion was  $4.5 \pm 0.4\%$  in patients sensitized only to spring pollens, while it was significantly higher ( $5.7 \pm 0.4\%$ ) in patients sensitized to both perennial allergens and spring pollens ( $P = 0.0146$ , Mann-Whitney  $U$  test) (Figure 2(b), Table 2). The blood cell eosinophil count showed the same reductive tendency (Figure 3(b)).

**3.5. Allergic Sensitization in Asthma.** Fifty-nine patients (46 adults, 13 children) had been previously diagnosed with asthma. The remaining 593 patients had not been diagnosed with asthma. Sensitization to any allergen was detected in 58% of patients with asthma (34/59). Twenty-six (44%) of 59 patients were sensitized to spring pollens (Table 3). Approximately half of the asthma patients (51%; 30/59) were sensitized to perennial allergens. Seven percent of patients with asthma (4/59) were sensitized only to spring

TABLE 3: Allergic sensitization in asthma.

Only spring pollens	4
Only fall pollens	0
Only perennial allergens	7
Spring and fall pollens	0
Spring pollens and perennial allergens	14
Fall pollens and perennial allergens	1
Spring and fall pollens and perennial allergens	8
No sensitization	25

pollen, while 16% (94/593) in patients without asthma were sensitized exclusively to these allergens. Thirty-seven percent of patients with a previous asthma diagnosis (22/59) were sensitized to both spring and perennial allergens, which was significantly higher than that observed in patients without asthma (20%; 117/593) ( $P = 0.0017$ , chi-square test).

Mean total serum IgE levels in patients with asthma were  $477 \pm 89$  IU/mL, while those in patients without asthma were  $224 \pm 27$  IU/mL ( $P = 0.0001$  compared to patients with asthma, Mann-Whitney  $U$  test). Blood eosinophil cell proportion in patients with asthma was  $5.4 \pm 0.6\%$ . In patients without asthma, the proportion was  $3.9 \pm 0.2\%$ . Blood eosinophil cell proportion in patients with asthma was significantly higher than those in patients without asthma ( $P = 0.008$ , Mann-Whitney  $U$  test).

#### 4. Discussion

Allergic sensitization, as diagnosed by the serum allergen-specific IgE level, does not always correspond with the patient's symptoms. We found that approximately twice as many patients were sensitized to both spring pollens and perennial allergens compared to patients sensitized only to spring pollens. However, many patients were asymptomatic to perennial allergens. Exposure to perennial allergens, such as house dust mite and cat and dog dandruff, is an important predisposing risk factor for asthma [4]. Previous diagnosis of asthma was largely related to serum IgE levels and blood eosinophil counts [5–7]. Even in nonasthmatic patients, airway responsiveness (assessed using methacholine [8]) is increased in some cases of allergic rhinitis, indicating an increased risk for asthma [9–11]. Sensitization to cat dandruff, dust mite, cockroach, and ragweed is an important predictor of airway hyperresponsiveness [12]. Airway hyperresponsiveness is strongly related to elevated total serum IgE levels, even in asymptomatic patients [5, 13]. In other words, total serum IgE level is considered an indicator of probable airway hyperresponsiveness or asthma. In our study, total serum IgE levels and blood cell eosinophil counts were significantly elevated in patients sensitized to both spring pollens and perennial allergens, as compared to patients sensitized only to spring pollens. Therefore, patients sensitized to both spring pollens and perennial allergens might be at greater risk of developing airway hyperresponsiveness or asthma.

Compared to adults, fewer children were sensitized only to spring pollens. Most children (approximately 80%) had

establishment of the modern child protection system. In 1988 Jasmine Beckford died, abused and malnourished despite 66 carers involvement in the case. The 1989 Children Act heralded the start of a new era, with the welfare of children a statutory priority, along with the right for children to have their voices heard. This was in accordance with the United Nations Convention on the Rights of the Child [5] that was also signed and made legal 1989. Despite such legislation, Victoria Climbié was tortured and murdered in 2000. The Laming Inquiry [6] made 108 recommendations that led to the Every Child Matters (ECM) Green Paper [7]. All these abuse cases had a lack of interagency communication and information sharing highlighted as prime failings. As such, the ECM paper focussed on bringing about integrated working. It promoted integrated working through the unification of services under the Children's Workforce Development Council [8] and a Common Core of Skills and Knowledge. A Common Assessment Framework was launched along with an information-sharing database called Contactpoint, shared tools for all professionals to use. Lead professionals were appointed to ensure that services were configured around the needs of individual children and Directors of Children's Services presided over multiagency Children's Trusts, ensuring the integration of services at a local authority level. The drive for integrated outcomes and services embodied in ECM became policy in the Children Act 2004 [9] and 2007 Children's Plan [10]. The stage had been set for integration on a scale never seen before. Kellett [11] surmises in her book that the agenda has brought benefits to England, increasing understanding of the need; to communicate, to plan holistically around the needs of the child, to intervene earlier in the lives of children and to listen to children.

Post the 2010 General Election, the Coalition Government revoked the need for statutory integration and the language of the previous government was banned [12]. Just as 'integration' seemed to be waning, year-on-year economic spending reviews drove a second wave of 'partnerships' and 'collaboration' resulting from the pressures of reduced budgets for services, rather than statutory requirements. Integration, collaboration and partnership were presented as the way ahead in a climate of economic paucity [13].

England was not alone in its drive for collaboration. The four home countries of the UK all adopted collaboration and integration. In Scotland the initiative was called 'Getting it Right for Every Child' [14], whilst Ireland's Ten Year Strategy [15] for children and young people contains a similar recognition for the need to integrate services around the needs of children. Wales also has a requirement for collaboration and partnership working to drive outcomes for children. The UK's fervour for

integration was perhaps not paralleled overseas. The Centre for British Teachers (CfBT) review of international integration found that:

Although a majority of countries and sub-national jurisdictions (34 of the 54 in the sample) have shown some level of commitment in policy terms to a joined-up or collaborative approach, very few have emphasised the centrality of integration along UK lines [16]. Alberta, Malta and the Netherlands were the notable exceptions as they did have integrated services like those found in the UK. All of the countries in the CfBT review were, however, found to be on a journey towards joined-up, collaborative or integrated services. [17]

Against this context, this study sought to understand the lived experiences of practitioners trying to deliver integrated care. There were multiple changes, restructures, guidance and tools, but the extent to which these helped practitioners to collaborate to provide integrated care was unknown. This research sought to understand what such collaborative practice looked like, and the extent to which it helped deliver integrated care. The professionals involved in all the cases above probably understood how to communicate with other agencies and are likely to have understood the necessity for integrated working, so why was it so evasive? The notion of 'agency' emerged from the research and was the central concept that explained what was happening. Agency refers to the awareness, choices and actions of an individual striving for what they need in the world. If extended to a group, rather than to an individual, the concept had potential to explain that the multiagency groups trying to achieve integration could be hindered by a lack of collective awareness, collective decision making or collaborative action. Whilst the concept emerged late in the research process, it is introduced here to frame the research. Professionals in the children's workforce with collaborative agency would be active subjects, able to make things happen, rather than passive objects to whom events happened [18]. Action does not necessarily mean activity – choosing to do nothing is an action [19]. What is important is that the collaborative team would assess the context, make choices, and use their power and capacities to interact with the world around them [19].

## Methods

The study commenced with a simple question about how people collaborated in the children's workforce, an interest that extended from the author's academic work teaching a Masters course in integrated service leadership. The four action research cycles iteratively developed and refined the research and led to the examination of agency in a collaborative context. The

(See figure on previous page.)

**Fig. 2** Automated counting of gp210 and pan-FG protein clusters per nuclear pore complex. **a** Overview showing pipeline modules sequence. **b** Influence of Gaussian blurring on structure of gp210 STED resolved structures. **c** Two color raw STED image of immunostained gp210 (red) and pan-FG (green) and images series produced after segmentation. **d** Zoom in image of segmentation results from CellProfiler window showing two neighbouring nuclear pores (left), gp210 clusters (middle), and pan-FG clusters (right). **e** Histogram plots showing quantitative segmentation results. **f** Current model of nuclear pore complex and two direction arrows connecting models with experimental results

In this paper, we mainly report the novelty and creativity of the procedure and to make pipelines available for public to use, modify and develop. We also suggest that image pre-processing e.g., applying bandpass filters, and critical inspection of SR images quality should always be carefully considered, clearly stated how it was carried out before publishing any quantification results. We

predict that future advancements in the field of user-friendly automated image analysis solutions optimized for SR microscopy will follow.

### Conclusion

The proposed computational image segmentation procedure is a novel method optimized for super resolution

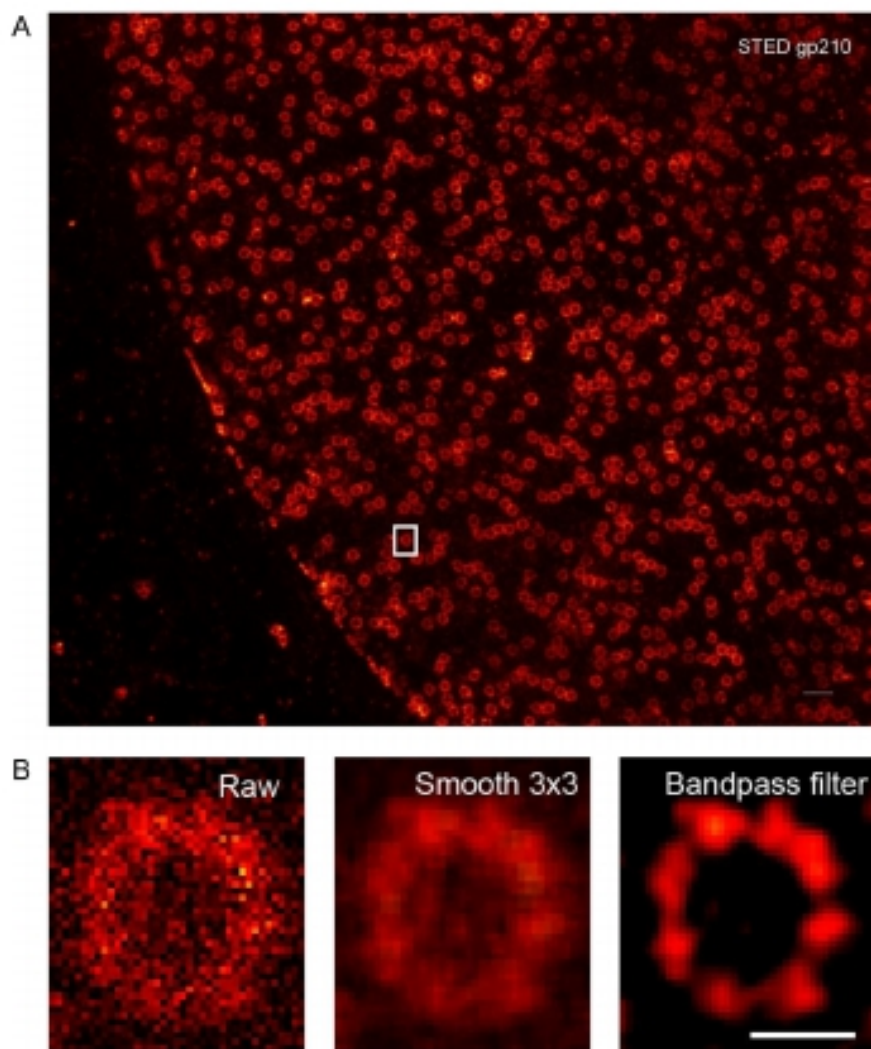


**Fig. 3** Enhancing image contrast by band pass filter improves visualization of gp210 clusters in noisy STED images. **a** Overview of single color STED image of gp210. **b** Close up on one nuclear pore (left), signal was enhanced by 3x3 smoothing (middle), or contrast enhanced by bandpass filter (right). Scale bar 500 nm in (a) and 100 nm in (b)

**Table 3** - Spine radiosurgery. Interventions and primary outcome descriptions from clinical trials registered at clinicaltrials.gov.

Study / Date started	Status	Design	Condition	Intervention	Primary outcomes
NCT01654068 (61) / Jul, 2012	Recruiting	Phase III	Spinal metastasis	1) 2-3 SM: 14 Gy SF 2) 1 SM: 14 Gy SF	Any skeletal-related event
NCT01223248 (52) / Oct, 2012	Recruiting	Phase III	Spinal metastasis	SR 24 Gy SF vs. SR, 27 Gy (HF)	Loco-regional control rates
NCT01290562 (62) / Jun 2011	Recruiting	Phase III	Spinal metastasis	20-24 Gy SF, or 20-24 Gy (HF) No prior RT or prior RT or Post-op	Local control: image / symptoms
NCT00573872 (63) / Dec 2007	Not recruiting (active)	Phase III	Spinal metastasis	Phase 1: 20-25 Gy (HF) / Phase 2: 9-24 Gy (SF)	TT: Safety
NCT01848510 (64) / Apr 2013	Recruiting	Phase II (2 arms)	Spinal metastasis	HF: 12 x 3 Gy + integrated boost 12 x 4 Gy / CRT 10 x 3 Gy	Local control
NCT02167633 (65) / Jul 2014	Recruiting	Controlled (2 arms)	MSCC	Decompression surgery plus CRT / SR 16 Gy SF	Ambulatory status
NCT00853528 (66) / Feb 2009	Not recruiting (active)	Phase I	Spinal metastasis	Maximum tolerated dose HF SR	Dose escalation
NCT00631670 (67) / Feb 2008	Completed	Controlled	Spinal metastasis	15 Gy SF / 25 x 2.8 Gy	Safety
NCT01525745 (68) / Jan 2012	Completed	Phase III	Spinal metastasis	SR HF / CRT 10 fractions	Pain control: NPPS
NCT01826058 (69) / Apr 2013	Recruiting	Phase III	MSCC	16-24 Gy SF / 21-36 HF	Neurologic response
NCT01254903 (70) / Dec 2012	Recruiting	Phase I	MSCC	18 Gy SF	Safety
NCT00922974 (9) / Nov 2009	Recruiting	Phase II: completed Phase III	Spinal metastasis	SR: 16 Gy SF / CRT 1 x 800 cGy	Pain control
NCT01752036 (71) / Mar 2013	Recruiting	Phase II	Spinal metastasis	SR: 30 Gy (HF)	Safety
NCT01347307 (72) / Sep 2008	Not recruiting (active)	Phase IV	Spinal metastasis	Benign: 12-16 Gy SF; 21-27 Gy HF Metastases: 14-25 Gy SF; 21-30 Gy HF	Tumor control
NCT01231061 (73) / Nov 2010	Completed	Phase III	Spinal metastasis	Arm 1: SR 24 Gy HF / SR 16 Gy SF	Pain control
NCT01950195 (53) / Jun 2013	Recruiting	Phase I	Spinal metastasis	SR + ipilimumab	Safety
NCT01624220 (74) / Jun 2012	Recruiting	Assignment	Spinal metastasis	SR + 4 gold seeds implanted	Safety

SR: spine radiosurgery; NPPS: numeric pain rating scale; TT: tomotherapy; QA: quality assurance; SF: single fraction; HF: hypofractionated; CRT: conventional radiotherapy; Post Op.: post operative; MSCC: metastatic spinal cord compression.

changes in tumor perfusion evaluated by dynamic contrast-enhanced (DCE)-MRI.

The Sidney Kimmel Comprehensive Cancer Center at Johns Hopkins University is currently conducting a phase I study that aims to assess the safety of prescribing either SR or stereotactic brain radiosurgery (SRS) in combination with ipilimumab (Bristol-Myers Squibb, New York, NY) to treat patients with newly diagnosed brain or spinal metastases from melanoma. The estimated enrollment is 30 patients, with a primary completion date of December 2016. The primary outcomes are a description of the number and severity of adverse events at 24 months and an assessment of the safety profile of SBRT with concurrent ipilimumab. The secondary outcomes include estimates of local control rates in the brain and spine at 24 months, determination of the systemic control rate and evaluation of progression-free survival (59). Recently published data have reported that using a combination of ipilimumab plus SRS for melanoma brain metastasis is well tolerated and associated with better loco-regional control and possibly better survival rates. However, there was a 20% rate of grade 3 or 4 toxicity using this treatment modality (53).

A retrospective series evaluated 106 metastatic renal cell carcinoma patients (55 spine and 51 brain metastases) who were treated with simultaneous standard sorafenib or

sunitinib (anti-angiogenic therapy) and stereotactic radiosurgery (SRS) or SR. The patients received an average dose of 20 Gy per lesion (range, 19–20 Gy) (54). The study showed no skin toxicity, neurotoxicity or myelopathy augment the adverse effects of anti-angiogenic therapy. Additionally, no treatment-related deaths or late complications were reported at 15 months. The local control rates for cerebral lesions at 12 and 24 months were 100% and 96.6%, respectively; for spinal lesions, the local control rates at 12 and 24 months were 94.1% and 90.4%, respectively. This series demonstrated that the use of SR / SRS plus anti-angiogenic therapy in this setting is safe and provides excellent local control.

The use of SR for metastatic tumors of the spine is safe and offers high local control rates. There are extensive data regarding pain control and local control; however, these data are mostly derived from retrospective and nonrandomized prospective series. Further studies are needed to determine appropriate SR fractionation schedules and clinical indications. Two RCTs (clinicaltrials.gov numbers NCT00922974 and NCT01223248) are ongoing and may provide the data needed to gain better insight into the factors that constitute optimal therapy. There is increasing interest in and a subsequent need to characterize combination drug therapy

In 2007, Yamada et al., using computed tomography, found that thin alveolar bone anteroposteriorly was associated with high mandibular plane angles and class III malocclusions [8].

More recently, Gracco et al., using computed tomography, confirmed the findings of the previously published two-dimensional studies which showed that the total thickness of the symphysis was greater in the short-face than in the long-face subjects [9] but did not make a connection between thin alveolus and clinical sequelae. In a study on cone-beam computed tomography (CBCT) evaluation of periodontal and bone support loss in extraction cases, the authors concluded that the buccolingual bone thickness was reduced after treatment in both groups, with no differences between the extraction and control groups [10].

It has been reported that CBCT can be used for highly accurate linear quantifications of external apical root resorption [11, 12]. In this retrospective study using CBCT data obtained as part of standard patient records, we evaluate the mandibular anterior alveolus of pretreatment and posttreatment records of adults. We not only describe a correlation between alveolus dimensions and skeletal facial type, but also measure changes to the mandibular alveolus and the lower incisor root length as a consequence of orthodontic treatment.

#### Specific aims

- (1) Compare the alveolar bone support (height and width) of mandibular central incisor in subjects with low, average, and high mandibular angle skeletal patterns before orthodontic treatment using CBCT.

- (2) Measure alveolar bone thickness change and root resorption of mandibular central incisor in the three skeletal patterns following orthodontic treatment.

#### Methods

##### Aim 1: Evaluation of mandibular anterior alveolar bone before orthodontic treatment

Committee on Human Research (CHR) approval was obtained from the Institutional Committee on Human Research (IRB 10-00564). Pretreatment CBCT images of 75 non-growing individuals, 25 in three groups: low-angle (sella-nasion to mandibular plane (SN-MP)  $\leq 28^\circ$ ), average-angle ( $30^\circ$ – $37^\circ$ ), and high-angle ( $\geq 39^\circ$ ), were analyzed. Consent to use individual CBCT data for research was obtained at the time of taking the CBCT. Buccolingual bone thickness was measured at the root apex, mid-root, and alveolar crest of the mandibular right central incisor. Inclusion criteria were non-growing, no orthodontic treatment before the initial CBCT scan, and no recorded craniofacial anomaly.

Using Anatomage Invivo5 CBCT software, sagittal slices were taken of the CBCT image through the middle of the root canal, at the midpoint of the long axis of the right central incisor (Fig. 1). From the sagittal slice of the center of the incisor, pretreatment measurements were taken for the buccolingual width at the apex and the alveolar crest (Fig. 2).

##### Reproducibility measurement

To test observer reliability, the measurements were repeated for ten subjects in each group, 1 month apart



**Fig. 1** Horizontal view through the mandibular dentition indicating the location of the sagittal slices to evaluate the alveolar bone and teeth. The slice through the center of the root canal (middle slice on the right) is then used for measurement of the tooth and surrounding bony support

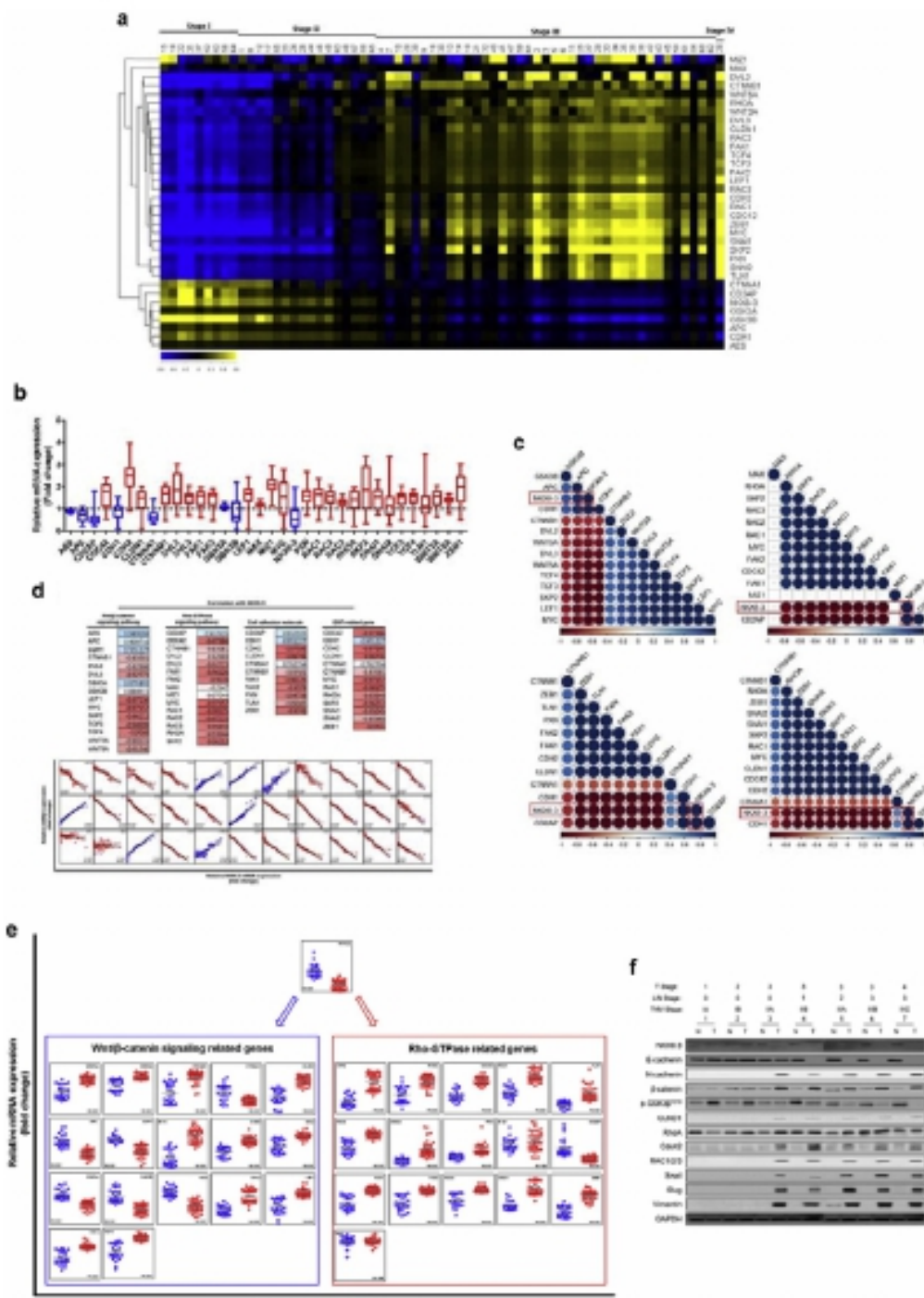


**Fig. 7.** NKX6.3 is negatively correlated with Wnt/β-catenin and Rho-GTPase signalling pathway genes in gastric cancer tissues. (a) Heatmaps demonstrate the expression ratios of NKX6.3, 33 Wnt/β-catenin and Rho-GTPase signalling-related genes, examined using quantitative real-time PCR in 65 gastric cancer tissues. On the scale bar, yellow indicates up-regulation and blue indicates down-regulation of mRNA compared to non-tumorous gastric mucosal tissues. Data are expressed as medians of three independent experiments. (b) Expression of NKX6.3 and 33 Wnt/β-catenin and Rho-GTPase signalling pathway genes in gastric cancer tissues compared to corresponding non-tumorous gastric mucosal tissues. Data are expressed as medians of three independent experiments. (c) Pearson correlation matrices revealed positive (blue) and negative (red) relationships between altered genes. (d) Pearson correlation with NKX6.3, Wnt/β-catenin, Rho-GTPase, cell adhesion and EMT-related genes (blue, positive correlation; red, negative correlation). (e) The effects of NKX6.3 on expression of 33 Wnt/β-catenin and Rho-GTPase signalling pathway genes in gastric cancer tissues with TNM stage (blue dot, stage I, II; red dot, stage III, IV). Data are expressed as medians from three independent experiments. (f) Expression of NKX6.3, E-cadherin, N-cadherin, β-catenin, p-GSK3β<sup>T216</sup>, CLND1, RhoA, Cdc42, Rac1/2/3, Snail, Slug and Vimentin protein expression in 7 gastric cancer tissues at different TNM stages and corresponding non-tumorous gastric mucosal tissues. Notably, N-cadherin, β-catenin, CLND1, RhoA, Cdc42, Rac1/2/3, Snail, Slug and Vimentin protein expression was increased in tumor tissues of gastric cancer patients with TNM stage II or III.

invasion. An excess of ROS generated during HR causes considerable cell damage, but plants can activate various mechanisms for the efficient scavenging of these transient augmentations in ROS. These include the non-enzymatic antioxidant systems, such as ascorbate and glutathione, and the enzymatic ROS-scavenging mechanisms in which catalase, peroxidase, ascorbate peroxidase, superoxide dismutase, glutathione peroxidases and peroxiredoxins participate. Transiently elevated ROS levels have also been considered as second messengers in plant, as they are perceived by different receptors, proteins or enzymes and seem to be involved with the regulation of phytohormones, such as ethylene (ET), salicylic acid (SA) and jasmonic acid (JA), which play important roles in plant-pathogen interactions [6].

After HR, a second kind of induced response against pathogen attack, the systemic acquired response (SAR), takes place, in which various defense genes are over- or down-regulated, mainly by intervention of SA, JA and ET [6]. Das *et al.* [7] showed that 552 genes were significantly differentially expressed between the *M. incognita*-infected and non-infected resistant cowpea CB46 plants and amongst the upregulated genes, there were those involved in metabolism (42.8%), genes coding for proteins with binding functions (25.3%) and genes involved in the interaction with the environment (15.8%), whereas those gene downregulated the code for proteins with binding functions (34.7%), metabolism (29.6%) and protein fate (20.3%).

The cowpea (*Vigna unguiculata* (L.) Walp.) legume is an important crop used as food mostly in tropical and semi-arid regions of the world. The dried seeds, leaves, immature seeds and fresh green pods are all consumed. However, the cowpea seeds represent the major form of utilization, because of their nutritional profile, particularly protein (20.3%–29.3%) and carbohydrate (55.6%–74.5%) contents [8]. The resistance of cowpeas to *M. incognita* resides on a single gene or locus, designated Rk, with alleles rk, rki, Rk, Rk2 and Rk3, which effectively inhibit the reproduction of *M. incognita* [9]. The cowpea genotype CE-31 is highly resistant to *Meloidogyne incognita* Race 3 [10].

The aim of this work was to analyze the differential accumulation of proteins in the roots of the resistant cowpea genotype CE-31 inoculated with *M. incognita* (Race 3) and non-inoculated control, using a 2D electrophoresis assay associated with mass spectrometry identification and gene expression analyses by reverse transcription-polymerase chain reaction (RT-PCR).

## 2. Experimental Section

### 2.1. Nematode Inoculum

The root knot nematode (RKN) inoculum was obtained from a population of *Meloidogyne incognita* (Race 3) isolated from susceptible cowpea plants (cv. Vita-3), growing in 1.5-L plastic pots containing exhaustive tap water washed river bottom sand that was previously mixed with humus (5:1, m/m) and autoclaved (121 °C, 30 min, 1.5 kgf/cm<sup>2</sup> (a kilogram-force per square centimeter)). Plants were maintained in a greenhouse, where the average temperature varied from 25 °C (night) to 35 °C (day), relative humidity (RH) from 55% (day) to 80% (night) and natural light *ca.* 700 μmol·m<sup>-2</sup>·s<sup>-1</sup> of photosynthetically active radiation (PAR) at the plant canopy. Irrigation was done daily with distilled water for up to 4 days after sowing, followed by irrigation (100 mL/pot) with 5-times diluted nutritive Hoagland and Arnon solution, as previously described [11]. Egg masses from *M. incognita* were isolated from galled cowpea roots using a stylet under a stereoscopic microscope (ausJENA, Jena, Germany). The egg masses were

### 7.2. Combinations with Other Transgenic Cytokines

Could other combinations of transgenic cytokines (besides GM-CSF plus IL-4 or GM-CSF plus IFN- $\gamma$ ) be effective in iDC reprogramming? As discussed before, GM-CSF is considered a critical factor for DC development under both steady-state and inflammatory conditions [22]. Upon binding to its cognate receptor, GM-CSF activates several intracellular signaling modules, including JAK/STAT, MAPK, PI3K and canonical NF- $\kappa$ B. Cytokines that are complementary to GM-CSF in the downstream STAT or ERK pathways are capable to further stimulate differentiation (IL-4) and activation/maturation of DCs (IFN- $\gamma$ ) [25], and result into different migratory properties. IDLV-mediated expression of GM-CSF plus IFN- $\gamma$  in human monocytes resulted in more activated iDCs that did not require *in vitro* treatment with additional maturation factors for optimal antigen presentation [43]. Since the multicistronic LV design is combinatorial, we can include additional cytokines that can complement GM-CSF and IFN- $\gamma$  such as IL-15 (for NK cell stimulation), IL-12 (for optimal Th1 activation), and so on. On the other hand, cytokines that are associated with tolerance (such as IL-10, TGF-B) could be also explored to maintain iDCs in a tolerogenic state.

### 7.3. Origin of Monocytes

Monocytes should be autologous to the cancer patient or allogeneic obtained from the same G-CSF mobilized donors donating CD34 $^{+}$  stem cells for HSCT. They should be highly purified as CD14 $^{+}$  cells (>95%). Donors for HSCT are strictly examined for HLA-compatibility, viral infections (HCV, HBV, HIV) and overall health status, making them a safe source of allogeneic monocytes.

### 7.4. Cell Manipulation *ex Vivo*

After monocytes are isolated by CliniMacs, the full GMP production requires only additional 28 h of *ex vivo* manipulation. Isolated CD14 $^{+}$  monocytes are pre-incubated in a bag system with recombinant huGM-CSF/huIL-4 for 8 h, transduced with LV at a low multiplicity of infection (MOI = 5) for 16 h in the presence of protamine sulphate as adjuvant, washed extensively, and cryo-preserved. The *in vitro* transduction of monocytes and the clinical grade of all cell product components provide high levels of safety and conformity. Since the transduction method is short, the emergence of malignant/transformed cells or replication competent lentivirus is unlikely to occur. Up to this date, no replication competent lentivirus (RCL) has been detected in cells transduced *ex vivo* with LV under GMP [46] and there is a current discussion at the FDA regarding RCL testing methods for viral batches. According to the FDA and EMA, cells that are transduced *ex vivo* for less than 4 days do not require RCL testing.

### 7.5. Ability to Proliferate

The transduced monocytes are post-mitotic cells and do not proliferate. *In vitro*, the differentiated DC senesce after 3–4 weeks and we have not observed any malignancy in mice administered s.c. with non-cryopreserved SmyleDCpp65 (maintained in observation for up to 9 months after administration).

of messenger RNA by the latest generation of sequencing technology (also known as RNA-Sequencing or RNA-Seq) is more straightforward, sensitive, and accurate in terms of the quantification of gene expressions, the systematic error rates and costs of said technology remain high compared to those of microarray technology, which has been in use for more than two decades (Mantione et al. 2014).

After collecting a global set of gene expressions, finding differentially expressed genes is the first step in deciphering the underlying mechanisms of a plant that copes with stress. In addition, biologists have recently been asking more about the systematic explanations of gene expression patterns. (e.g., Atkinson and Urwin 2012; Hahn et al. 2013; Priest et al. 2014). Such inquiries have motivated the advancement of gene set analysis and the utilization of microarray data to make inferences regarding genetic networks. Gene set analysis concerns the disturbed gene sets instead of individual genes whereas the gene sets of interest are predetermined (e.g., the co-expressed genes, the genes in the same category of the gene ontology, the genes involved in the same metabolic pathway, etc.) (Kaeber et al. 2014, 2015; Rest et al. 2016). Network inference, which is the focus of this study, links genes with edges that indicate potential associations to depict the possible interactions among the chosen set of genes (Todaka et al. 2012; Rasmussen et al. 2013; Nakashima et al. 2014).

The construction of a correlation network is one approach that can be taken after a microarray experiment, while conducting a weighted gene co-expression network analysis (WGCNA) is another. The former can be accomplished by computing the pairwise Pearson correlation coefficients of genes and connecting a given gene pair if the Pearson correlation coefficient exceeds a user-specified threshold (Song et al. 2012). The choice of the threshold, however, might be very subjective, and different thresholds result in networks with different topologies (Borate et al. 2009). A WGCNA, however, preserves all possible edges in the network but assigns different weights to them instead. By clustering the genes with high-weight edges, WGCNA is able to determine the modules (gene sets) of genes highly associated with each other according to the observed expression data. In this study, we further extend the application of WGCNA in three directions:

1. Instead of using the correlation coefficient as the measure of the association between genes, we choose the coefficient of intrinsic dependence (CID).
2. We explore stress-specific modules by conducting the analysis of variance on the expression levels of the Eigen genes representing the gene modules and

by comparing the edge weights of the stress-specific modules.

3. A biplot is introduced to visualize the stress-specific modules for convenience in further interpretation.

Along with long-term development of the technology, a huge amount of results from a wide range of microarray experiments has been accumulated. As of August 18, 2016, data from a total of 179 microarray experiments had been included in the *Arabidopsis* Information Resource (TAIR) database. Typical experiments have consisted of several treated samples under a particular condition and several controlled samples as the background of comparison for the reasons of purification and simplicity. However, analyzing the expression patterns under one stressed condition versus those under control conditions can only reveal a corner of a huge puzzle. One is not able to depict an overview of the entire system or of the interactions between the impacts caused by different stress sources on the living organisms. Therefore, in this study, we combine all possible samples from different stress conditions and perform a meta-analysis of the gene regulatory network on the combined dataset.

To that end, the coefficient of intrinsic dependence (CID), instead of the typical Pearson correlation coefficient, is used to measure the association between genes because the Pearson correlation coefficient only measures the linearity of the gene associations. However, past studies (Liu 2005; Liu et al. 2009) have shown that a nonlinear relationship between the expressions of two associated genes might occur in some cases. The CID does not require distributional and functional assumptions regarding the data and is useful for analyzing noisy microarray data. Relatedly, while systematic errors are well controlled in highly developed microarray technology, samples from different experiments contribute noise to each other when a meta-analysis is conducted due to the fact that the expression patterns from different experiments have a wide range of variation (Ramasamy et al. 2008; Campain and Yang 2010). The CID had been applied to investigate gene regulatory events incorporating the Galton-Pearson correlation coefficient (Liu et al. 2009, 2012), to identify associations among multivariate variables (Liu and Tsai 2013), and to select relevant features on a step-by-step basis according to their importance in relation to the target variable (Hsiao and Liu 2016). In this study, we strictly followed the definition and methodology of CID described in Hsiao and Liu (2016) and focus on utilizing the CID in measuring the magnitude of association in general between genes based on microarray gene expression data.

A CID matrix is used to construct the weighted gene co-expression network produced by a WGCNA.

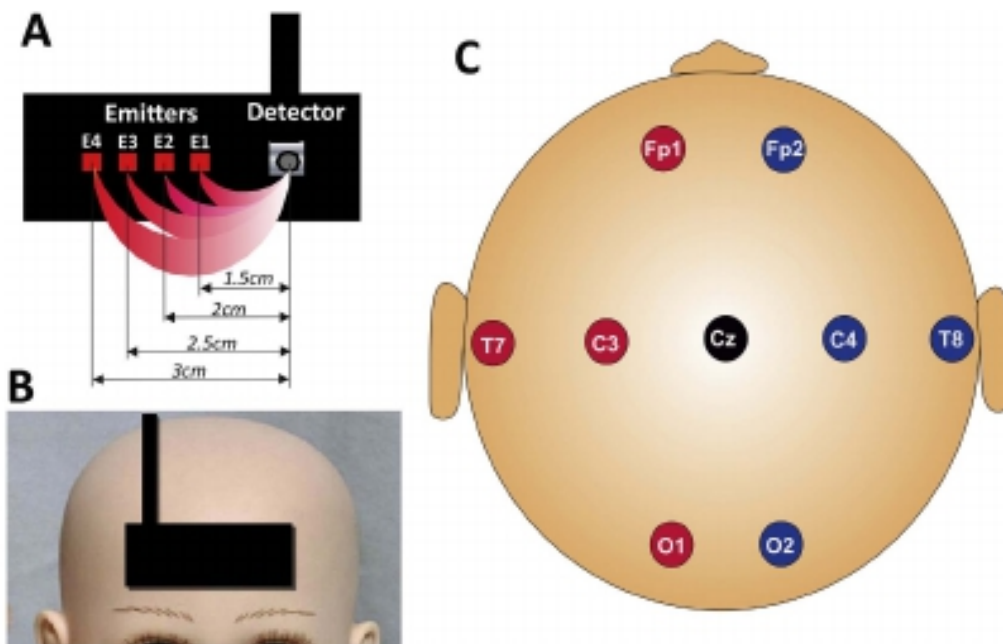


**Fig. 1.** EEG and optical imaging acquisition data

A–B: A patch comprising four pairs of optical fibers (one fiber for each wavelength in each pair) and a detector has been positioned in the middle of the forehead. The four channels (A1–A4) differed in the distance between the emitter and the detector (15, 20, 25 and 30 mm for channels A1 (D–E1), A2 (D–E2), A3 (D–E3) and A4 (D–E4), respectively).

C: 9 electrodes were disposed according to the 10–20 system, with a frontal reference.

neurotransmitter deficiency and deteriorating general condition. Seven of the 9 patients displayed manifestations during monitoring, and 6 had spasms in clusters. The seventh child had a partial seizure (in the absence of typical spasms) and was thus excluded from the study.

### 3.2. EEG and clinical data

The patients' clinical characteristics, interictal and ictal EEG data are summarized in Table 1 (for more details, see Supplemental data).

Patient #1 presented with idiopathic infantile spasms, beginning at the age of 6 weeks. After 6 months of standard treatment (vigabatrin and hydrocortisone), the patient was spasm free and the clinical outcome was normal. The five other patients presented symptomatic infantile spasms as the result of heterogeneous etiologies. All of them had poor neurological evolution and developmental delay.

Patient #2 presented symptomatic infantile spasms as the result of left temporo-parietal polymicrogyria.

Patient #3 was delivered by emergency cesarean section at 40 weeks of gestation, following the observation of acute fetal distress syndrome and perinatal anoxo-ischemia.

Patient #4 presented with symptomatic infantile spasms as a result of a neurotransmitter deficiency (suggested by a very low level of 5-methyltetrahydrofolate in the cerebrospinal fluid).

Patient #5 was delivered by cesarean section after 35 weeks of gestation, following the observation of intra-uterine growth retardation. A mitochondrial cytopathy, a metabolic disorder, was diagnosed, with a confirmed lack of complex IV in muscle and liver biopsies. The last patient (Patient #6) presented with Group B *Streptococcus* meningoencephalitis at the age of 1 month. The infection had caused severe anoxic and ischemic damage. A CT scan revealed almost complete destruction of the parenchyma and a thin cortical ribbon resulting in a very large porencephalic cyst (Fig. 2).

### 3.3. fNIRS data

Between 6 and 29 typical spasms (for patients #1 and #6, respectively) were recorded using simultaneous EEG/fNIRS. Each spasm lasted for 1 or 2 s, and the interval between spasms ranged from 6 to 110 s.

Combined EEG-multidistance fNIRS revealed changes in [HbO], [Hb] in all children (Fig. 3). In all children other than the one with a large porencephalic cyst, two hemodynamic phases were extracted from the optical signals. The first hemodynamic phase consisted of parallel changes in [HbO], [Hb], with a peak within 5 s of the onset of deltoid activity – suggesting that spasm was associated with initial changes in cerebral blood volume (CBV). In all patients other than the child with the large porencephalic cyst (patient #6), this was followed by NVC (i.e. concomitant opposite changes in [HbO] and [Hb]). The NVC was positive in 4 out of 5 patients (i.e. an increase in [HbO] and a decrease in [Hb]), with a peak 10 s after the peak in phase 1. The NVC was negative (i.e. a decrease in [HbO] and an increase in [Hb]) in the patient with a mitochondrial cytopathy (patient #5). In patient #6, only a small, late (5 s) but significant increase in both [HbO] and [Hb] was observed (Fig. 3).

#### 3.3.1. Cortical specificity of the hemodynamic response

To determine whether or not these hemodynamic changes had a cortical origin, we took advantage of the multidistance optical probe's ability to scan the optical changes at different tissue depths. In all patients and in both phases, the absolute amplitude of changes in [HbO] and [Hb] increased with the emitter-detector distance (Fig. 4A). The normalized [HbO] range increased with the source-detector distances increment (Fig. 4B).

This confirms the cortical origin of the hemodynamic response and suggests that the channels with the lowest emitter-detector distance (scanning superficial, non-cortical structures) are barely affected by the changes in chromophore concentration occurring in the deeper, cortical layers.

ter Dr Taylor's death in 2010, the Panel reconvened under the leadership of Dr Robert Black, Professor of International Health at Johns Hopkins, and has participated in the final set of recommendations that constitute the final article in this series [32].

When the review began in 2006, the focus was exclusively on child health (that is, the health of children in their first 5 years of life). With support from USAID and the Gates Foundation between 2013 and 2016, it became possible to expand the scope of the review to maternal health. Thus, we have now renamed the overall effort a review of the effectiveness of CBPHC in improving MNCH.

### Goals of the review

The goal of this review is to summarize the evidence regarding what can be achieved through community-based approaches to improve MNCH. The health of mothers, neonates and children as a measurable outcome is defined here for our purposes as the level of mortality, serious morbidity, nutritional status, or coverage of proven interventions for mothers, neonates and children in a geographically defined population. The review focuses on interventions and approaches that are carried out beyond the walls of health facilities that serve populations of mothers, neonates and children living in geographically defined areas.

The review consists of an analysis of documents describing research studies, field projects, and programs (collectively referred to in this series as projects) that have assessed the impact of CBPHC on MNCH. Altogether, the findings comprise a comprehensive overview of the global evidence in using CBPHC to improve MNCH. In addition, the review describes the strategies used to deliver community-based interventions and the role of the community and community health workers in implementing these interventions. In addition, the review seeks to understand the context of the projects – where they were implemented and by whom, where the funding came from, for how long, what size of population was served by the project, and what additional contextual factors might have influenced the project outcomes – as well as the methodological quality of the assessment.

The questions which the review seeks to answer are:

- How strong is the evidence that CBPHC can improve MNCH in geographically defined populations and sustain that improvement?
- What specific CBPHC activities improve MNCH?
- What conditions (including those within the local health system) facilitate the effectiveness of CBPHC and what community-based approaches appear to be most effective?
- What characteristics do effective CBPHC activities share?
- What program elements are correlated with improvements in child and maternal health?
- How strong is the evidence that partnerships between communities and health systems are required in order to improve child and maternal health?
- How strong is the evidence that CBPHC can promote equity?
- What general lessons can be drawn from the findings of this review?
- What additional research is needed?
- How can successful community-based approaches for improving MNCH be scaled up to regional and national levels within the context of serious financial and human resource constraints?
- What are the implications for local, national and global health policy, for program implementation, and for donors?

### METHODS

The Task Force and the Expert Panel agreed on the following definition of CBPHC:

CBPHC is a process through which health programs and communities work together to improve health and control disease. CBPHC includes the promotion of key behaviors at the household level as well as the provision of health care and health services outside of health facilities at the community level. CBPHC can (and of course should) connect to existing health services, health programs, and health care provided at static facilities (including health centers and hospitals) and be closely integrated with them.

immature male (44047, S13) both migrated to the same approximate area east of South Carolina, U.S. However, the immature male consistently used comparably warmer waters ( $SST > 20^{\circ}\text{C}$ ) than the immature female ( $SST < 20^{\circ}\text{C}$ ). Considering the expansive geographic range, which inherently includes a wide temperature range, and the directed selection of certain temperatures, particularly by males, it is unlikely that blue shark seasonal migrations are solely motivated by temperature-related physiological constraints. While foraging and thermoregulation may influence expanded depth use off the shelf, these hypotheses are confounded by the added effect of simultaneously undergoing migration.

Though the mechanisms of migration are poorly understood in pelagic animals, it is reasonable to assume that blue sharks must receive and interpret navigational cues during migrations covering thousands of kilometers. One hypothesis suggests that migratory sharks, such as scalloped hammerheads (*Sphyrna lewini*), dive below the thermocline to ascertain magnetic cues necessary to navigate [39, 73–75]. High-resolution data collected from the mature female contained dives into the mesopelagic zone during its 3765 km migration, suggesting deep, directed dives may be related to long-distance movements [76]. Additionally, blue sharks may assess bathymetric formations or detect undersea landmarks during dives, particularly the continental shelf ledge, potentially relevant to north-south movements [37]. If bathymetric cues are causative factors of depth selection during migration, sharks would exhibit greater depth use during periods of directed long-distance movement. In addition to navigational cues, the functionality of deep dives may fully, or in part, pertain to a number of alternative behaviors, such as predator avoidance, conspecific interactive behavior, or following prey [70, 76–78]. Distinct hypothesis testing of the biological significance of deep diving was beyond the scope of this study, and continues to challenge scientists, despite recent advances of tracking technologies [76]. Unlike the mature males in this study, immature males remained in the northwest Atlantic, not undergoing long-distance movements, and consistently selected significantly shallower depths, indicating that net displacement is related to deeper depths used by migratory sharks.

#### Long-distance movements and comparison to Atlantic migration models

All blue sharks tagged in the northwest Atlantic moved southeast off the continental shelf (Fig. 7) [15, 25, 37]. Females did not exhibit mating wounds, however, if mating is closely followed by migration away from the shelf aggregation, it is possible that these females had not yet mated at the time of capture. One immature female traveled south to the tropics, and its tag reported from

an area north of The Bahamas in July. The other immature female was tagged in southern waters in the spring, but made a net northeast migration to approximately 1600 km from the continental shelf aggregation in August. This further suggests that females may not return to the continental shelf in the spring and summer. Contrastingly, Atlantic blue shark movement hypotheses suggest males undergo northern migrations in the spring and annually return for summer residence on the continental shelf [22, 25]. An immature male (44047, S13), migrated northeast during March and April, and its tag released less than 500 km from the continental shelf aggregation, which supports annual philopatry to the shelf aggregation by males (Fig. 7). Remaining long-distance tracks concluded in February, prohibiting the assessment of springtime movements. However, current movement models hypothesize that northern movements do not commence until after February, which potentially explains the absence observed in our data [22]. Results from this study align with current blue shark migration hypotheses; however, both are inherently biased towards locations with large fishing efforts (i.e., northwest Atlantic). As such, future studies should aim to address deficiencies in geographical coverage.

Atlantic blue shark migration theory is especially deficient in describing mating areas or overlapping habitat for mature males and females. A single stock and an unstructured gene pool (authors' unpublished data) suggest an overlapping spatial area characterized by mixing of adults. This, and other studies, have observed that some mature blue sharks migrate south to the Caribbean in the winter and spring [15, 36, 77, 78]. Additionally, all immature male sharks tracked in this study remained in the North Atlantic, not undergoing long-distance migrations, further supporting the hypothesis that mature blue sharks migrate to lower latitudes for reproductive purposes. Though unobserved at the New England study site, two adult female blue sharks with fresh mating wounds (personal observation  $\leq 2$  weeks) were captured discretely in The Bahamas. One female, migrated approximately 3704.1 km to the Mid-Atlantic Ridge, roughly 600 km southwest of the Azores. Mark-recapture data from the western Atlantic proves that a small percentage of tagged individuals make transatlantic migrations to the Azores, coasts of Portugal and Spain, Canary Islands, African coast, and Cape Verde Islands [22]. Sightings of neonate blue sharks and mature females in advanced stages of pregnancy suggest Azorean waters may serve as a springtime parturition area [36]. However, the spatio-temporal gaps in mark-recapture data allow the potential that some portion of the population uses Caribbean waters as a stop-over or interim area before crossing the Atlantic to pupping grounds. If fresh mating wounds indicate pregnancy, it is possible the aforementioned female captured in The

Fluid shear stress is confirmed as one of the dominant factors among mechanical factors [49,51,57]. The barrier function and stability related to the permeability of the vessel wall were examined for various values of flow rate, shear stress, transmural pressure, and average luminal pressure, and among different parameters, the fluid shear stress was determined as the most dominant factor [57]. Shear stress lowers the permeability and ultimately increases stability by narrowing vascular cells. Moreover, shear stress inhibits sprouting from the vascular wall through nitric oxide action, even in the presence of interstitial flow and vascular endothelial growth factor (VEGF) gradient (Figure 2a.1) [20].

Interstitial flow also plays a major role in vessel development. In particular, the sprouting behaviors are very different depending on the direction of interstitial flow acting upon the sprouting vessel (Figure 2a.2) [45]. Sprouting from existing vascular networks is most active in the reverse direction of interstitial flow. Additionally, given the gradient of the angiogenic factor with interstitial flow together, their influence on vasculatures may be greater. For instance, sprouting in both reverse interstitial flow and positive VEGF gradients showed a significant number of activated filopodial protrusions into the gel, but sprouting in both forward interstitial flow and negative VEGF gradients showed dilated morphologies [12].

Some attempts have been made to examine the effects of cellular mediators that respond to mechanical stimuli. For example, ECs regulate their morphology such as the polarization and alignment through the mechanism mediated by small GTPase RhoA in response to shear stress [58]. Furthermore, by culturing RhoA-blocked HUVECs in microfluidic devices, it has been confirmed that the RhoA-mediated mechanism plays a major role in VEGF-driven vascular development, especially extension, under shear flow [59]. Additionally, histone deacetylases have been identified to stimulate MMP14 expression in response to interstitial flow and VEGF [60].

### 3.2. Chemical Factors

Angiogenic growth factors are intensely involved in angiogenesis as the name suggests [1]. VEGF is the most important growth factor for blood vessel formation as it promotes EC migration and proliferation through VEGF receptor-2 signaling [61,62]. Most importantly, VEGF determines the direction of angiogenic sprouting by guiding the filopodial protrusion to a higher concentration of VEGF [2,63]. Other angiogenic growth factors such as platelet-derived growth factor (PDGF), transforming growth factor beta 1 (TGF- $\beta$ 1), and angiopoietin (Ang-1) enhance the stabilization of the vessel wall through different cellular mechanisms [2]. There have also been attempts to quantify the role of various angiogenic factors when they are selectively or simultaneously introduced [20,64].

The generation of a concentration gradient of angiogenic factors is crucial in vessel formation as it guides the directions of vasculogenesis or sprouting (Figure 2b). A linear profile of chemical concentrations can be formed in the hydrogel because the diffusion rate of a molecule is much lower in hydrogel than in the cell medium [65]. Therefore, various shapes of gradient profiles can be obtained by varying the configurations of microfluidic channels [9]. For example, a relatively simple device with a single gel channel between two media channels [66,67] or a device with two gel channels between three media channels can generate the linear gradient profiles across the gel channels [65]. In addition, a device with a gel scaffold enclosed by three channels can form two profiles of gradients in two orthogonal directions (Figure 2b) [21]. In these ways, different aspects of sprout formation can be examined under the gradients of each angiogenic factor.

### 3.3. Biological Factors

The examples of EC types commonly used for vascularization on chips are HUVECs, human microvascular ECs (HMVECs), and human artery ECs (HAECs). Although the differences in their functional characteristics regarding angiogenesis are poorly understood, there has been a study comparing the functional angiogenic ability of HAECs and HUVECs using microfluidic systems [68]. In the 3-D microenvironment, HAECs exhibited excellent angiogenic potential compared to HUVECs through particular mRNA upregulation, which was not revealed in a 2-D culture system. There have also been some attempts to increase physiological relevance by culturing organ-specific cell lines

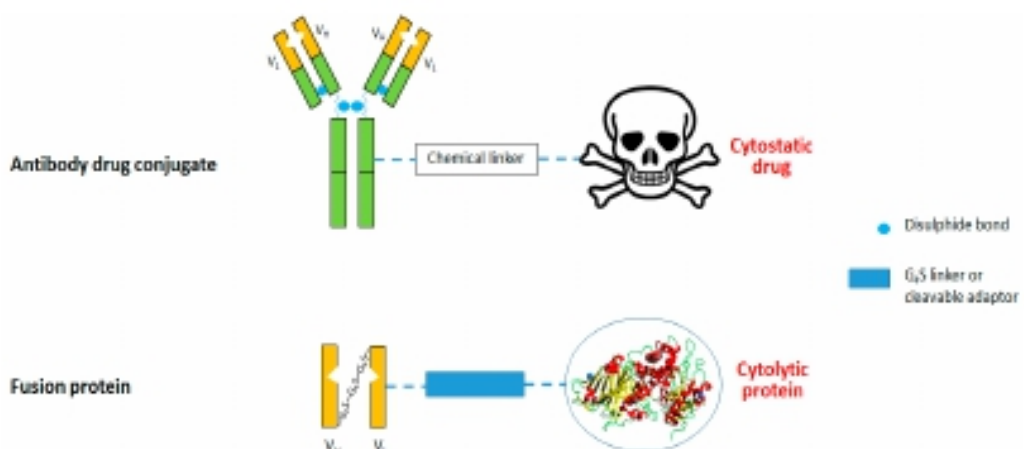


**Figure 2.** Immunotoxins comprising antibodies linked to an anti-cancer agent. The scFv portion (yellow frame) of the monoclonal antibody (green frame) retains antigen specificity and binding capacity. Antibody drug conjugate: 1st generation (monoclonal antibody) and 2nd generation (scFv), conjugated to a chemotherapeutic drug; Fusion protein: 3rd generation (bacterial/viral effector) and 4th generation (human effector). Recombinant proteins enable the introduction of a variety of adaptor peptides to facilitate cytosolic delivery (blue rectangle).

### 3. Anti-CSPG4 Immunotoxins

Protein-based ITs consist of a disease-specific antibody fragment (targeting domain) recombinantly fused to a cytotoxic protein, such as Exotoxin A (effector domain) separated by intramolecular peptide linker [38]. In general, ITs exhibit acceptable tumor penetration and serum stability. Improved tumor penetration is achieved by using a tumor-targeting scFv (or nanobody) [36] and the smallest truncated form of a protein toxin that still retains its cytotoxicity. This approach yields a much smaller drug molecule than the first-generation full-length mAb and full-length toxin versions. Protein engineering technology has also been used to design ranges of peptide linker variants, including linkers with elements that facilitate production and purification, as well as those that improve serum stability and influence intracellular routing of the IT [39–41].

Exotoxin A (ETA) is a potent cytotoxic protein produced by *Pseudomonas aeruginosa*. ETA consists of three functional domains: a cell binding domain (I), an intracellular membrane translocation domain (II) and an adenosine diphosphate (ADP)-ribosylating domain (III) [42]. Domain III is responsible for the toxicity of ETA by inactivating elongation factor 2 (EF-2) via ADP-ribosylation, interrupting protein production and inducing cell death with great potency (theoretically, a single molecule ETA can induce full arrest of cellular biosynthesis). Already in the early stages of IT development, ETA was recognized as a cytotoxic effector domain with promising anticancer activity [43]. The intrinsic cell binding and translocation capacity of full-length ETA ensures cytosolic delivery of the toxic domain III. However, these same characteristics of ETA are also the source of tumor specificity problems, as non-specific cell binding leads to off-target toxicity. This problem was largely overcome by employing a truncated form of ETA (ETA') which lacks its cell binding Domain Ia [44], such as used in an ETA'-based IT targeting MSCP (CSPG4) recently generated by Brehm and co-workers [21] using a novel bacterial expression system [45].

In the following sections, we will provide a short overview of CSPG4-targeting scFv-fusion proteins which have been preclinically evaluated for efficacy towards various refractory cancer types, in particular in rhabdomyosarcoma (RMS), a soft-tissue sarcoma occurring in young children (in the form of embryonal RMS, eRMS) as well as older children and adults (typically alveolar or pleomorphic RMS, aRMS or pRMS) [46]. The different forms of RMS have distinct molecular origins and can occur in a wide range of tissues, hence a combination of conventional therapeutic modalities is recommended

## POLICY PAPER

# How do Policy and Institutional Settings Shape Opportunities for Community-Based Primary Health Care? A Comparison of Ontario, Québec and New Zealand

Tim Terbansel\*, Fiona Miller†, Mylaine Breton‡, Yves Couturier‡, Frances Morton-Chang†, Toni Ashton\*, Nicolette Sheridan\*, Alexandra Peckham†, A Paul Williams†, Tim Kenealy\* and Walter Wodchis†

Community-based primary health care describes a model of service provision that is oriented to the population health needs and wants of service users and communities, and has particular relevance to supporting the growing proportion of the population with multiple chronic conditions. Internationally, aspirations for community-based primary health care have stimulated local initiatives and influenced the design of policy solutions. However, the ways in which these ideas and influences find their way into policy and practice is strongly mediated by policy settings and institutional legacies of particular jurisdictions. This paper seeks to compare the key institutional and policy features of Ontario, Québec and New Zealand that shape the 'space available' for models of community-based primary health care to take root and develop. Our analysis suggests that two key conditions are the integration of relevant health and social sector organisations, and the range of policy levers that are available and used by governments. New Zealand has the most favourable conditions, and Ontario the least favourable. All jurisdictions, however, share a crucial barrier, namely the 'barbed-wire fence' that separates funding of medical and 'non-medical' primary care services, and the clear interests primary care doctors have in maintaining this fence. Moves in the direction of system-wide community-based primary health care require a gradual dismantling of this fence.

**Keywords:** community-based primary health care; Canada; New Zealand; policy; institutions

## Introduction

Community-based primary health care describes a model of service provision that is oriented to the population health needs and wants of service users and communities, and has particular relevance to supporting the growing proportion of the population with multiple chronic conditions. The ideal of community-based primary health care incorporates an understanding of primary health care which places an emphasis on the principles of equity, community partnership while addressing social determinants of health [1, 2]. Community-based primary health care also involves a realignment of health system resourcing, emphasising the need for more 'upstream' approaches to prevention and care in the management of chronic conditions, and inter-professional approaches to service delivery. Thirdly, community-based primary health care

recognises the need for action outside the health sector to implement health agendas and inter-sectoral approaches to health [3].

Internationally, aspirations for community-based primary health care have stimulated local initiatives and influenced the design of policy solutions. However, the ways in which these ideas and influences find their way into policy and practice is strongly mediated by policy settings and institutional legacies of particular jurisdictions.

Both the Canadian Institutes of Health Research and the New Zealand Health Research Council identified the importance of building cross-jurisdictional policy-relevant research regarding community-based primary health care. A resulting collaboration between researchers in New Zealand and the two most populous provinces in Canada (Québec and Ontario) Implementing Integrated Care For Older Adults With Complex Health Needs (iCOACH) is examining the implementation of local integrated care initiatives considering policy, organizational, provider and patient and informal carer perspectives.

In this article, we outline the key policy and institutional features of New Zealand and the Canadian provinces of Ontario and Québec that shape the opportunities for

\* University of Auckland, NZ

† University of Toronto, CA

‡ University of Sherbrooke, CA

Corresponding author: Tim Terbansel, Associate Professor (tterbansel@auckland.ac.nz)

**Table 5** Spearman correlations coefficients between SRS-22 domains and 4 factors of 16PF-APQ

SRS domains		Function	Pain	Body Image	Mental Health	SubtotSRS-22
16PF-APQ	Rule-Consciousness	.35 <sup>*</sup> <i>p</i> = .03	.44 <sup>**</sup> <i>p</i> = .001	.40 <sup>*</sup> <i>p</i> = .01	.30 <i>p</i> = .06	.61 <sup>**</sup> <i>p</i> = .000
	Independency	-.22 <i>p</i> = .21	-.34 <sup>*</sup> <i>p</i> = .04	-.51 <sup>**</sup> <i>p</i> = .002	-.54 <sup>**</sup> <i>p</i> = .001	-.60 <sup>**</sup> <i>p</i> = .000
	Vigilance	-.3 <i>p</i> = .7	-.33 <sup>*</sup> <i>p</i> = .04	-.42 <sup>**</sup> <i>p</i> = .007	-.36 <sup>*</sup> <i>p</i> = .02	-.45 <sup>**</sup> <i>p</i> = .003

<sup>\*</sup>*p* < .05; <sup>\*\*</sup>*p* < .01

Taking coping style into account, doctors may advise patients to join some group activities, avoiding the possible tendency to stay at home studying all day. Indoor activities, such as using internet social networks, make social interactions much less threatening, but that is only communicating and not a real connection with the real world. In a determined moment, shy teens "have to log off the computer and log on life" [27]. Physiotherapy in a group could be useful as well as all kinds of activities allowing personal expression such as theater, free dance, or any group activities (scouting, trekking, etc.).

In the correctional study about Personality and HRQOL, Body Image, Mental Health domains, and the overall HRQOL had the highest ( $r > .5$ ,  $p < .01$ ) negative correlations with Independence while correlated positively with Rule-Consciousness. These correlations surprised us as intuitively we would think the opposite: the more the person is independent, the better Body Image, Pain HRQOL, and Mental Health s/he has. Interpreting the results, we have to take into account that independence is a proper theme in adolescence when teenagers struggle to grow up, find their identity, and become adults [28]. As a consequence, Independence and Rule-Consciousness are core themes for adolescents. An adolescent, who is developing his independence in the building of his identity, has more difficulties than an obedient adolescent in accepting his/her body image and with his/her mental health.

Furthermore, significant correlations between Vigilance and HRQOL, specifically Pain, Body Image, and Mental Health, were found. A vigilant person appears suspicious, jealous, or envious while his/her opposite is a trusting person, who is collaborative, not competitive, and interested in the others. So, the correlation could be interpreted as follows: a vigilant person could suffer, comparing his/her body with the others and having more difficulties in accepting his/her body than a trusting person.

We suggest taking account of the results of adolescents' Body Image and Mental Health in SRS-22; also, other variables, such as *Independence*, *Rule-Consciousness*, and *Vigilance*, may influence them.

However, this study lacks a control group of patients without scoliosis. Further research will be needed to consider a control group of healthy adolescents not coming from the hospital and to enlarge the sample size;

besides, it would be interesting to repeat the study with a representative sample of adults, focusing on the relationship between HRQOL and personality.

## Conclusions

In conclusion, adolescents with scoliosis were introverted and self-sufficient. Introversion did not differ for the magnitude of the deformity, for the brace treatment, or for the perception of the trunk. Adolescents with better Body Image and Mental Health were less vigilant but less Independent.

The assessment of the introversion trait should have a consequence in the planning of specific rehabilitation programs for the treatment of adolescents with scoliosis. Rehabilitation programs have to integrate physiotherapy exercises with psychosocial activities. These last activities help adolescents in expressing themselves and sharing their experiences with the others, in order to create interests beyond their inner world and improve their social relationship.

## Abbreviations

16PF-APQ: 16 Personality Factors-Adolescent Personality Questionnaire; HRQOL: Health-related quality of life; SRS-22: Scoliosis Research Society-22 Questionnaire; TAPS: Trunk Appearance Perception Scale

## Acknowledgements

There was no acknowledgment for this study.

## Funding

There was no funding for this study.

## Availability of data and materials

Please contact the author for data requests.

## Authors' contributions

ED has made substantial contributions to the conception and design, data measurement, recruitment of patients, data analysis, and interpretation and has been involved in drafting the manuscript. JSR has made substantial contributions to the conception and design, acquisition of data, recruitment of patients, data analysis and interpretation, and drafting of the manuscript and given final approval of the version to be published. JB has revised it critically and gave important suggestions for intellectual contents. All authors read and approved the final manuscript.

## Ethics approval and consent to participate

This study was approved by the Clinical Research Ethics Committee (CEIC) at Hospital Vall d'Hebron Research Institut

## Consent for publication

Not applicable